

CFD Analysis on Thermal Performance of Nanofluids in Electric Vehicle Battery



P. L. Palaniappan, T. T. K. Lokeswar, V. Adhitya, and R. Harish

Abstract As electric vehicles are becoming more popular, thermal management systems for batteries have become an important aspect of keeping the temperature and performance of the batteries under check. Exposure to extreme or higher temperatures might lead to the reduction in maximum voltage and the durability of the battery. Thus, an efficient way of thermal management is required for good performance. This research paper deals with the modelling and simulation of a thermal management system of batteries, which makes use of nanofluids as a cooling medium. The battery is modelled as a cylindrical body with isothermal temperature surrounded by nanofluid as cooling medium. Water is considered as a base fluid and parametric study is conducted using different nanoparticles such as aluminium, aluminium oxide and graphene. The volume fraction of the nanofluid is varied between 2 and 8%. Monodispersed spherical particles of uniform size are referred to as nanoparticles. By taking into account the impacts of natural convection, the problem is treated as a three-dimensional incompressible unstable flow. The problem is investigated by plotting the streamline, temperature, velocity and pressure contours. The findings show that the type of nanofluid used and its volume percentage can have a substantial impact on the flow and heat transfer characteristics of batteries. The findings of this study will aid in determining the ideal nanofluid combination for increasing heat transfer rate.

Keywords Battery · Nanofluids · Enhancement

1 Introduction

Batteries have now become an inevitable part of our day-to-day life. They have their applicability in a wide range of fields from consumer electronics to electrical vehicles. The most widely used batteries in the present-day world are lithium-ion batteries. Lithium-ion batteries have profound use because of their rechargeable capabilities.

P. L. Palaniappan · T. T. K. Lokeswar · V. Adhitya · R. Harish (✉)
School of Mechanical Engineering, Vellore Institute of Technology, Chennai,
Tamil Nadu 600127, India
e-mail: harish.r@vit.ac.in

© The Author(s), under exclusive license to Springer Nature Singapore Pte Ltd. 2023
V. K. Singh et al. (eds.), *Advances in Thermal Sciences*, Lecture Notes
in Mechanical Engineering, https://doi.org/10.1007/978-981-19-6470-1_7

During both periods of charging and discharging, there is dissipation of heat from their surfaces which exposes the battery continuously to high temperatures. This may affect the operating conditions and efficiency of the battery. Constant operation at excessive temperatures dwindles the performance of the batteries and also fast tracks the deterioration process thus reducing the battery's lifespan. Additionally, there is a possibility of the heat generation value of the battery exceeding the amount of heat dissipation to the surroundings. This phenomenon known as thermal runaway can create a domino effect with the internal battery temperature rising exponentially bringing about a rise in battery current. This hike in temperature in any single battery can set about affecting other batteries in the close vicinity. Besides the excessive temperature, the large disparity in the temperatures inside the battery package could potentially lead to irregular current densities and battery decay. All these issues arise the need for a proper thermal management system of a battery to transmit the excess heat to the surroundings and maintain the battery at optimal temperatures.

Ahmed et al. [1] used a single-phase model in an inclined square enclosure with buoyancy-driven flow to examine the utilization of CuH_2O nanofluid. The two surfaces under consideration are a cold obstacle and a circular cylinder with unsteady state convection taking place between the surfaces. Jilte et al. [2] investigated two techniques of cooling component arrangement: liquid filled battery cooling systems and liquid circulated battery cooling systems. The two-cooling mediums considered are water and alumina-water nanofluid and inspect the improvement in cooling performance by addition of nanoparticles. Harish and Sivakumar [3] examined the turbulent thermal convection flow with the heat and cold sources attached to the walls of the cubical enclosure using nanofluids. A transient, three-dimensional, two-phase mixture model was developed with the values of Grashof numbers varied to compute the results. Karimi et al. [4] investigated the use of phase change composites to increase the heat transfer rate of cylindrical lithium-ion batteries. The different phase change material (PCM) used were copper, silver and iron oxide, and the computed results were weighed up with metal matrix of PCM. Alipanah et al. [5] studied the outcome of various geometrical and operating conditions on the battery surface temperature which is the vital aspect of BTMS. The cooling media considered were octadecane and gallium and aluminium foams with different porosities were saturated with these mediums to determine the increase in the thermal conductivity values.

Jilte et al. [6] studied the characteristics of a thermal management system which uses nano-enhanced phase change materials for better heat transfer. In this study on addition of nanoparticles to phase change materials, it was observed that after a certain time, the addition of nanoparticles enhanced the heat absorption characteristics of the material. Huo et al. [7] using lattice Boltzmann method investigated the thermal management system which was based on nanofluid medium. He used aluminium oxide as the nanoparticles suspended in water as the cooling medium and conducted the analysis on a cylinder with uniformly distributed constant heat source. Mondal et al. [8] worked on the thermal management system and investigated on the efficacy of nanoparticles. In this study, different nanoparticles were tested on the battery with different flow configurations. Kiani et al. [9] looked into pure water and nanofluid battery thermal control systems. The system was used in conjunction with phase

change material (copper foam filled with paraffin wax). Singh et al. [10] looked at the thermal conductivity of various nanofluids to see how diverse their applications are.

Liu et al. [11] studied about the effectiveness of nanofluid on the mini-channel thermal management in lithium-ion battery. It is observed in this paper that the addition of nanofluid shows great influence on cooling effect in fluids with lower thermal heat conductivity especially on engine oil. The addition of nanoparticle to base fluid shows a very good thermal management performance as they control the maximum cell temperature. Kiani et al. [12] investigated the use of nanofluid, metal foam and phase change material in the hybrid thermal control of lithium-ion batteries. In this paper, the authors have shown that nanofluid cooling system is very much effective in thermal management when compared to that of water-cooling system during stressful operating conditions of the battery. It is observed in this paper that nanofluid cooling system extends the battery's operation time. Nasir et al. [13] studied about the nanofluid heat pipe in managing the temperature of electric vehicle lithium-ion battery. When aluminium oxide nanofluid with a volume fraction of roughly 0.015 is used as a working fluid in a heat pipe, the overall thermal resistance is reduced by 15% when compared to water filled heat pipes. Wiriyasart et al. [14] investigated the nanofluid thermal management system for battery cooling modules in electric vehicles. It is observed that the battery surface temperature reduces up to 27.6% when compared to that of conventional battery cooling modules. It is also found that the cooling effect of the coolant would increase drastically if the concentration of the nanoparticles suspended in the coolant is higher. Wu et al. [15] investigated the nanofluid-based battery thermal management system using lattice Boltzmann method. The authors have observed 6.5% decrease in the temperature of the battery if we use nanofluid with 0.06 volume fraction.

Majority of the earlier papers involves the investigation of effects of usage of nanofluids in distinct shapes. To the best of authors' knowledge, there is a lack of study on the comparison of different nanofluids' utilization in battery thermal systems and singling out the best ones. Thus, this paper studies the use of aluminium, Al_2O_3 and graphene in a simulated battery thermal environment and figuring out the most efficient nanofluid particle. A three-dimensional model is developed in an unsteady state environment to determine the different required characteristics. Through the alteration of different volume fraction values, the heat transfer characteristics of various nanofluids are investigated. Similar investigations were performed in [3, 16–19].

2 Methodology

The designed model of the presented problem comprises of an unsteady state flow of nanofluids enclosed in an enclosure. The nanofluids are considered to be incompressible and viscous. The base fluid to be used is water with the nanoparticles suspended in them. The three different nanoparticles under consideration are aluminium, alumina and graphene. The battery is in cylindrical shape with a diameter of 14 mm and

height of 50 mm. This cylindrical battery surface generates heat uniformly over its surface. Thus, the boundary condition is set to be constant wall temperature of 85 °C at the outer surface of the cylinder. The acceleration due to gravity is taken in the conventional direction and is set as 9.81 m/s². The thermophysical properties are presumed to be constant.

2.1 Governing Equations

The conservation equations for mass, momentum and energy equations of the fluid are as follows:

$$\frac{\partial \rho_f}{\partial t} + \nabla \cdot (\rho_f u) = 0 \quad (1)$$

$$\frac{\partial (\rho_f u)}{\partial t} + \nabla \cdot (\rho_f u u) = \nabla \cdot p + \nabla \cdot (\mu_f \nabla u) \quad (2)$$

$$\frac{\partial (\rho_f C_{pf} T)}{\partial t} + \nabla \cdot (p_f C_{pf} T u) = \nabla \cdot (k_f \nabla T) \quad (3)$$

where ρ_f represents the density of fluid, μ_f indicates the dynamic viscosity, C_{pf} depicts the specific heat of the fluid and k_f represents the thermal conductivity of the fluid. The other parameters like the velocity, time and temperature are denoted by u , t and T , respectively. The assumptions taken under this study are incompressible fluid flow and steady state heat transfer.

$$\frac{\partial k}{\partial t} + U_j \frac{\partial k}{\partial x_j} = P_k \frac{\partial}{\partial x_j} \left[(v + \sigma_k v_T) \frac{\partial k}{\partial x_j} \right] \quad (4)$$

$$\frac{\partial \omega}{\partial t} + U_j \frac{\partial \omega}{\partial x_j} = \frac{\partial}{\partial x_j} \left[(v + \sigma_\omega v_T) \frac{\partial \omega}{\partial x_j} \right] + 2(1 - F_1) \sigma_{\omega 2} \frac{1}{\omega} \frac{\partial k}{\partial x_i} \frac{\partial \omega}{\partial x_i} \quad (5)$$

Equation (4) and (5) denote the turbulent kinetic energy equation and diffusion equation, respectively, where K is the kinetic energy, ν represents the kinematic viscosity of the nanofluid, ν_T represents the turbulent viscosity and U_j indicates the velocity in the domain.

σ_w denotes the empirical constants. ω and P_k variables in the equation are the turbulent dissipation rate and production of turbulent kinetic energy, respectively.

2.2 Thermophysical Properties

According to the requirements pertaining to the required study, the effective density, heat capacitance. Thermal conductivity and absolute viscosities of the nanofluids were computed based on the following formulas with different volume fraction values under consideration. The values are computed using the formulas and presented in Table 1

$$\rho_{nf} = (1 - \emptyset)\rho_f + \emptyset\rho_p \tag{6}$$

$$(\rho C_p)_{nf} = (1 - \emptyset)(\rho C_p)_f + \emptyset(\rho C_p)_p \tag{7}$$

$$\frac{k_{nf}}{k_f} = \frac{(k_p + 2k_f) - 2\emptyset(k_f - k_p)}{(k_p + 2k_f) + \emptyset(k_f - k_p)} \tag{8}$$

$$\mu_{nf} = \frac{\mu_f}{(1 - \emptyset)^{2.5}} \tag{9}$$

$$(\rho\beta)_{nf} = (1 - \emptyset)(\rho\beta)_f + (\emptyset)(\rho\beta)_p \tag{10}$$

$$\alpha_{nf} = \frac{k_{nf}}{(\rho C_p)_{nf}} \tag{11}$$

Table 1 Property values of different nanofluids

Nanofluids	Volume fraction	Density (Kg/m ³)	Viscosity (Pa. s)	Heat capacity (J/kgK)	Thermal conductivity (W/mK)
Aluminium	0.02	1034	0.000936	4015.016673	0.642768328
	0.04	1068	0.00099	3855.38809	0.681054605
	0.06	1102	0.00104	3705.609546	0.720954813
	0.08	1136	0.0011	3564.79662	0.762573202
Aluminium oxide	0.02	1059	0.00094	3938.91407	0.641203288
	0.04	1118	0.00099	3718.354204	0.677796832
	0.06	1177	0.00104	3519.906542	0.715864647
	0.08	1236	0.0011	3340.404531	0.755497657
Graphene	0.02	1025.4	0.00094	4031.178077	0.643056194
	0.04	1050.8	0.00099	3884.316711	0.681654448
	0.06	1076.2	0.00104	3744.38766	0.721893065
	0.08	1101.6	0.0011	3610.911402	0.763878884

where φ refers to the volume fraction of the nanoparticle. The subscripts in the equation p , f and nf represent the thermal capacity, μ represents the dynamic viscosity, β means the thermal expansion coefficient and α depicting the thermal diffusivity. Table 1 represents the thermophysical properties of three different nanofluids under different volume fraction.

2.3 Simulation Modelling

Fluent in Ansys software was used to run the simulation. We created a cylinder 15 mm in diameter and 50 mm in length. It was enclosed in an enclosure of 100 mm in all six directions. The created model was meshed further with the default size. Further, all the sides of the enclosure and cylinder was named using the named selection. Next step was carried on the Fluent environment. The enclosure fluid was defined here using the nanofluid properties taken from Table 1. The surface of the cylinder is defined with a constant wall temperature of 333 K (60 °C), and the fluid is taken to be at 293 K (20 °C). All the residuals of velocity, momentum and energy are set to values of 1e-06. Calculations were carried out for a total of 1000 iterations. The flow in this simulation is considered to be incompressible and turbulent. Further, the values of convective heat transfer coefficients, surface heat flux values are taken from the reports. Contours for temperature pressure and velocity are plotted with the count of contours to be 1000. The maximum temperature was taken from the contour plotted in Fig. 1.

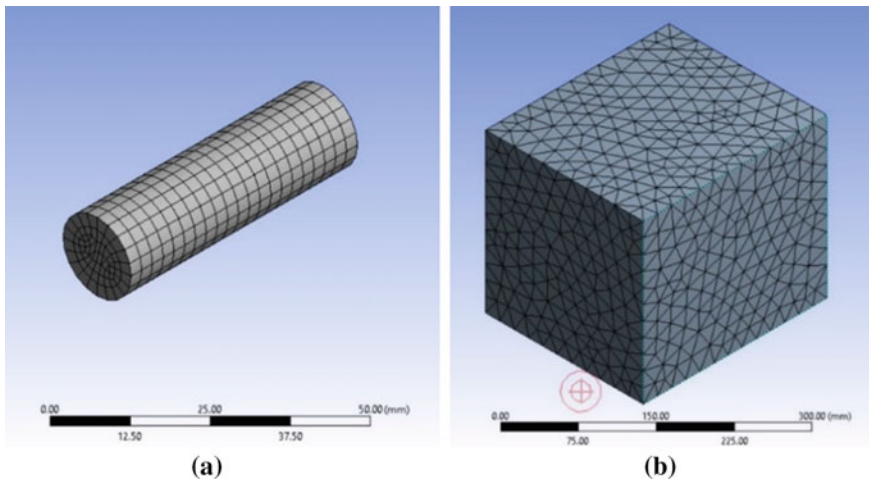


Fig. 1 Meshing of **a** cylinder in the enclosure **b** the enclosure

3 Result and Discussions

Temperature, velocity and pressure contours of all the 12 simulations are calculated. Figure 2a represents one such temperature distribution contour of aluminium-water nanofluid with a volume fraction of 6%. In this scenario, the temperature decreases as the distance from the battery increases, forming a concentric rings pattern. The temperature varies from a maximum temperature of 333 k on the surroundings with a temperature of 293 K. The temperature is conducted in the initial stage from the solid cylinder to surrounding fluids whereby afterwards the convection takes over and the temperature near the fluid is convected to the low temperature surroundings. Figure 2b represents the velocity distribution of the same case. Due to convection, the particles near the fluid get the energy and diffuse towards the walls of the enclosure which can be seen in the visualization as small patches. Figure 3 represents the pressure distribution of the same case. All other values' temperature, velocity, and pressure contours were found to be similar to Figs. 2a, b and 3 accordingly.

The velocities of the nanofluids are highest near the heat source, which is the cylindrical battery, in the early periods. These high-energy particles propagate towards the wall surfaces as the transient heat transfer continues. Thus, after a period of time, the higher velocities are seen to be concentrated towards the enclosure fences as seen in Fig. 2b. As observed from Fig. 3, the pressures are spotted to be maximal near the vicinity of the top surfaces. This is a result of the buoyancy forces acting

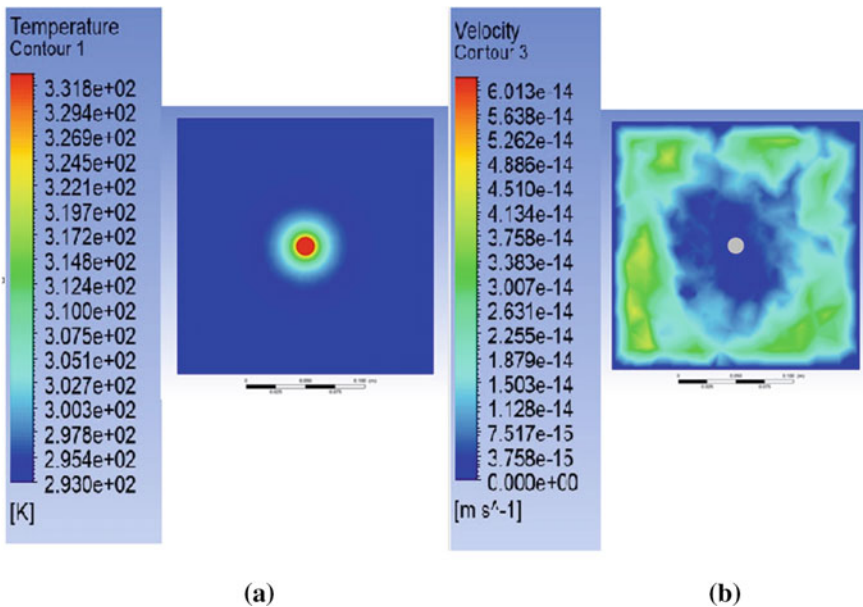


Fig. 2 a Temperature distribution contour of (aluminium–water) with $\phi = 6\%$ b Velocity distribution of (aluminium–water) with $\phi = 6\%$ at the base of the cylinder

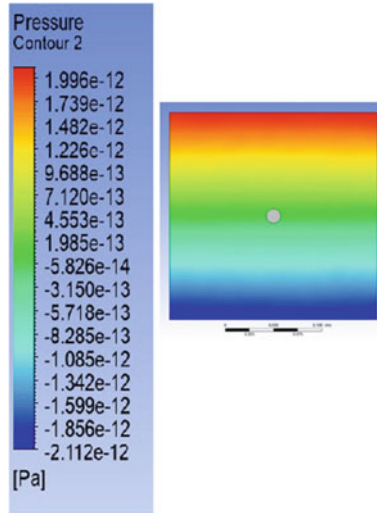


Fig. 3 Pressure distribution contour of (aluminium–water) with $\phi = 6\%$

on the nanofluid molecules. The particles absorb this heat and grow lighter as the temperature of the molecules rises due to the heat generated. As a result, a significant concentration of molecules may be found near the upper parts, resulting in higher-pressure results. Similarly, lower pressures are seen in the lower surface where a lesser concentration of nanofluids can be identified.

The fluctuation of the heat transfer coefficient with volume fraction is depicted in Fig. 4a. It is observed that the line graph for the variation is found to be increasing linearly with the addition of nanoparticles. When the volume percentage was increased from 2 to 4%, the heat transfer coefficient increased by 4.67 per cent. Subsequently, there was an increase of 4.3% and 4.52% increase in h value from 4 to 6% and 6% to 8%. Figure 4b represents the total heat flux variation with volume fraction. The pattern found here is that the value of surface heat flux increases momentarily as the volume fraction of nanoparticles in nanofluids increases, implying that more heat is transported per unit area as the volume fraction of nanoparticles grows.

The fluctuation of the heat transfer coefficient with the volume fraction for alumina-water nanofluid is shown in Fig. 5a. An exact increasing trend was observed in the case of heat transfer coefficient with the value jumping from $63.75 \text{ W/m}^2\text{K}$ to $72.46 \text{ W/m}^2\text{K}$ on varying the volume fraction from 2 to 8%. Similarly, a positive slope is observed in case of total surface heat flux in Fig. 5b varying from 2858.501 W/m^2 to 3249.34 W/m^2 on addition of nanoparticles. Figure 6 indicates that the heat transfer coefficient and total surface heat flux increases with increase in volume fraction for graphene-water nanofluid.

Simulation of graphene-water nanofluid was carried out with different nanoparticles concentration, and the results were plotted on a graph. An increasing slope is

Fig. 4 Variation of **a** heat transfer coefficient (W/m^2K) and **b** total surface heat flux (W/m^2) with volume fraction of aluminium-water nanofluid

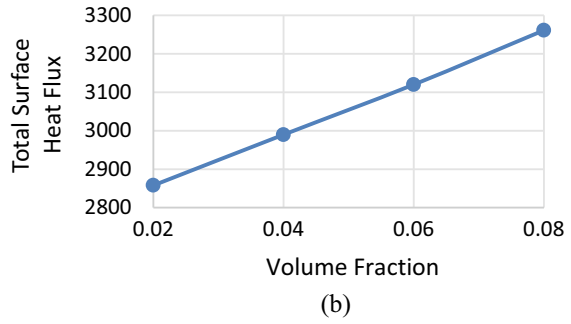
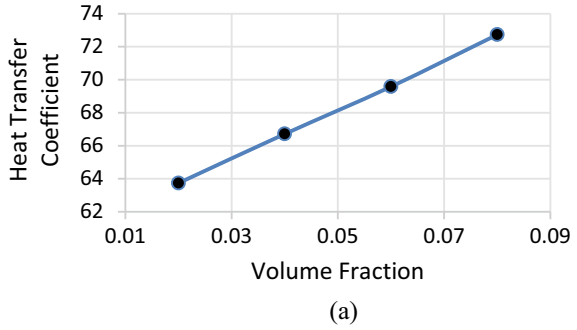


Fig. 5 Variation of **a** heat transfer coefficient (W/m^2K) and **b** total surface heat flux (W/m^2) with volume fraction of alumina-water nanofluid

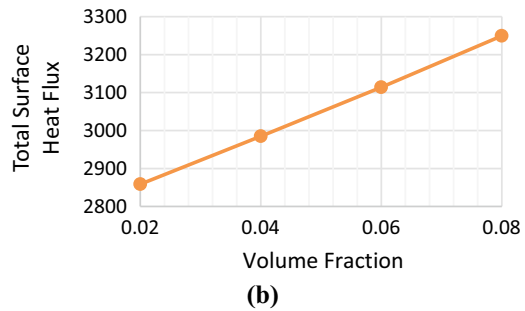
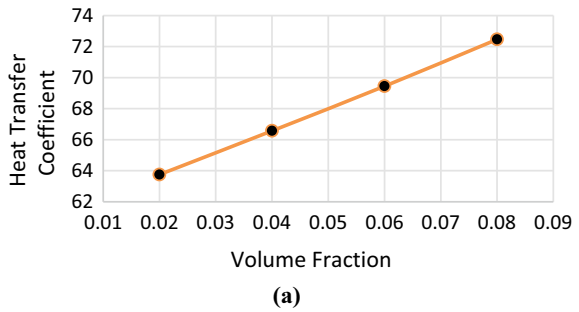
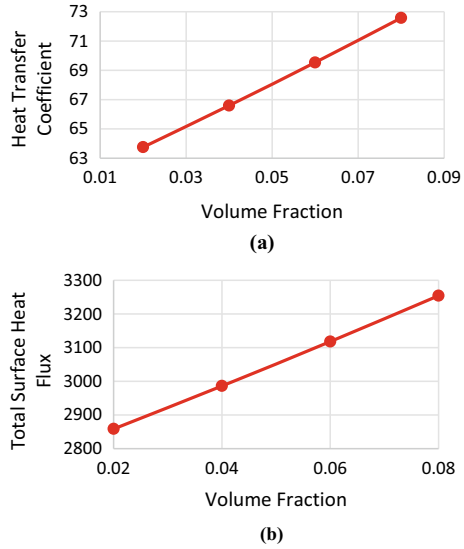


Fig. 6 Variation of **a** heat transfer coefficient (W/m^2K) and **b** total surface heat flux (W/m^2) with volume fraction of graphene-water nanofluid



observed in case of heat transfer coefficient on increasing the nanoparticle concentration. On the other hand, the total surface heat flux increases on increasing the nanoparticle concentration. On average the heat transfer coefficient increases by a percentage of 4.41% for 2% increase in nanoparticle concentration. In case of total surface heat flux, it increases by an average of 4.25% on rise of 2% rise in the nanoparticle concentration. Figure 7 represents the comparison aluminium-water, alumina-water and graphene-water nanofluids combination's fluctuation in the coefficient of heat transfer with the increase in nanoparticle concentration. On comparing on all the values obtained in the simulation, it can be noted that aluminium has the highest coefficient of heat transfer comparing to aluminium oxide and graphene. Aluminium with a volume fraction of 8% exhibited the highest of all heat transfer coefficients with a value of 72.73 W/m^2K . It can also be noted from the line graphs that the value of h increases with the rise in nanoparticle concentration for all the three cases. Figure 8 depicts the increase in the coefficient of convective heat transfer on increasing the volume fraction by 2 percentage. It was observed that a change of 4.5% on average increase on increasing the volume fraction by 2%.

4 Conclusion

- This work establishes a lithium-ion battery model of a nanofluid-based battery thermal management system to keep the battery temperature within safe limits. On a cylinder with a constant wall temperature, the validation is carried out.

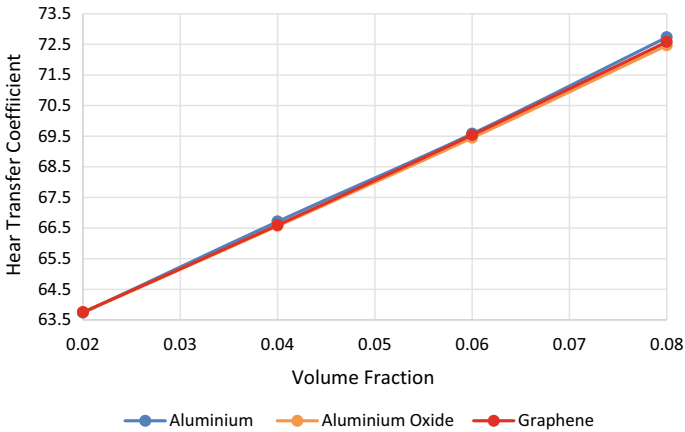


Fig. 7 Comparison of all the above mentioned nanofluids

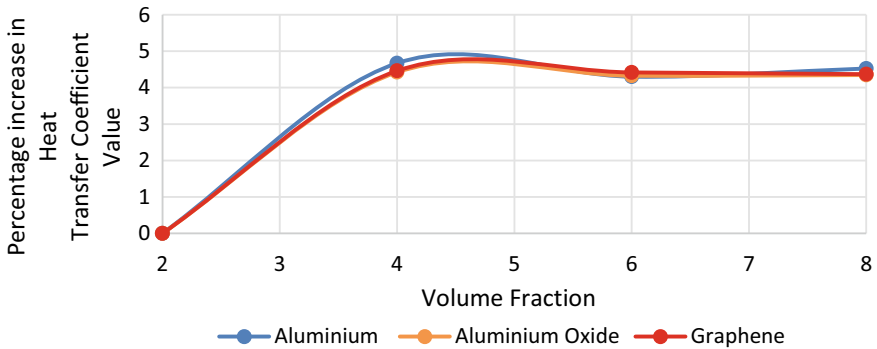


Fig. 8 Percentage increase of heat transfer coefficient on increasing the value of nanoparticle concentration

- The cooling qualities have been investigated, and it has been discovered that the cooling features improve as the percentage of nanoparticles in the nanofluid increases.
- Out of the three nanofluids, aluminium-water nanofluid exhibited a higher convective heat transfer coefficient. The highest heat transfer coefficient of $72.73 \text{ W/m}^2\text{K}$ is observed on the Al-water nanofluid with 8% volume fraction of aluminium which signifies its better ability of cooling and maintaining a lower temperature on the surface of a battery.
- In the variation of total surface heat flux with volume fraction of nanoparticles, it is concluded that with the increase of nanoparticle concentration, the amount of heat transferred per unit area has increased on the surface which shows its ability to be added along with base fluid to enhance the cooling capacity.

- Similarly, a maximum heat flux of 3261.166 W/m^2 was observed in case of aluminium–water nanofluid with a nanoparticle concentration of 8%. Thus, the nanofluids can be used in order to increase the rate of heat transfer to the surroundings from the surface of the battery to maintain it at optimal temperatures.

References

1. Ahmed E, Elshehaby H (2018) Buoyancy-driven flow of nanofluids in an inclined enclosure containing an adiabatic obstacle with heat generation/absorption: effects of periodic thermal conditions. *Int J Heat Mass Transf* 124:58–73
2. Jilte D, Kumar R, Mohammad H (2019) Cooling performance of nanofluid submerged versus nanofluid circulated battery thermal management systems. *J Cleaner Prod* 240:118131
3. Harish R, Sivakumar R (2021) Turbulent thermal convection of nanofluids in cubical enclosure using two-phase mixture model. *Int J Mech Sci* 190:106033
4. Karimi G, Azizi M, Babapoor A (2016) Experimental study of a cylindrical lithium-ion battery thermal management using phase change material composites. *J Energy Storage* 8:168–174
5. Alipanah M, Xianglin L (2016) Numerical studies of lithium-ion battery thermal management systems using phase change materials and metal foams. *Int J Heat Mass Transf* 102:1159–1168
6. Jilte R, Asif A, Satyam P (2021) A novel battery thermal management system using nano-enhanced phase change materials. *Energy* 219:119564
7. Huo Y, Rao Z (2015) The numerical investigation of nanofluid based cylinder battery thermal management using lattice Boltzmann method. *Int J Heat Mass Transf* 91:374–384
8. Mondal B, Lopez CF, Mukherjee PP (2017) Exploring the efficacy of nanofluids for lithium-ion battery thermal management. *Int J Heat Mass Transf* 112:779–794
9. Kiani M, Omiddezyani S, Houshfar E, Miremadi SR, Ashjaee M, Nejad AM (2020) Lithium-ion battery thermal management system with $\text{Al}_2\text{O}_3/\text{AgO}/\text{CuO}$ nanofluids and phase change material. *Appl Therm Eng* 180:115840
10. Singh AK (2008) Thermal conductivity of nanofluids. *Def Sci J* 58(5):600
11. Liu H, Chika E, Zhao J (2018) Investigation into the effectiveness of nanofluids on the mini-channel thermal management for high power lithium-ion battery. *Appl Therm Eng* 142:511–523
12. Kiani M, Ansari M, Arshadi AA, Houshfar E, Ashjaee M (2020) Hybrid thermal management of lithium-ion batteries using nanofluid, metal foam, and phase change material: an integrated numerical–experimental approach. *J Therm Anal Calorim* 141(5):1703–1715
13. Nasir FM (2019) Nanofluid-filled heat pipes in managing the temperature of EV lithium-ion batteries. *J Phys: Conf Ser* 1349(1). IOP Publishing
14. Wiriyasart S, Hommalee C, Sirikasemsuk S, Prurapark R, Naphon P (2020) Thermal management system with nanofluids for electric vehicle battery cooling modules. *Case Stud Therm Eng* 18:100583
15. Wu F, Rao Z (2017) The lattice Boltzmann investigation of natural convection for nanofluid based battery thermal management. *Appl Therm Eng* 115:659–669
16. Janjanam N, Nimmagadda R, Asirvatham LG, Harish R, Wongwises S (2021) Conjugate heat transfer performance of stepped lid-driven cavity with $\text{Al}_2\text{O}_3/\text{water}$ nanofluid under forced and mixed convection. *SN Appl Sci* 3(6):1–13
17. Harish R, Sivakumar R (2021) Effects of nanoparticle dispersion on turbulent mixed convection flows in cubical enclosure considering Brownian motion and thermophoresis. *Powder Technol* 378:303–316
18. Harish R (2018) Buoyancy driven turbulent plume induced by protruding heat source in vented enclosure. *Int J Mech Sci* 148:209–222
19. Harish R (2018) Effect of heat source aspect ratio on turbulent thermal stratification in a naturally ventilated enclosure. *Build Environ* 143:473–486